AN ABSTRACT OF THE THESIS OF

Terry Allen Nelsen   for the   M. S.
(Name)   (Degree)

in   Oceanography   presented on *Nov. 30, 1970*
(Major)   (Date)

Title: DENSITY SEPARATION OF CLAY MINERALS

Abstract approved: Redacted for privacy

G. Ross Heath

Illite, chlorite, montmorillonite and kaolinite, as well as natural marine sediments and mixtures of the standards were subjected to density separation by centrifugation in a linear heavy-liquid gradient.

The density layers yielded by centrifugation were recovered and analyzed by X-ray diffraction. Separates were not monomineralic but rather were polymineralic usually with minerals of invarient density, such as quartz, in more than one layer. This incomplete separation is attributed to insufficient centrifugation time. The X-ray character of minerals of variable density changes in such a way as to suggest increased crystallinity with depth in the density gradient.

Although several samples were known to contain montmorillonite, none of the density layers showed X-ray evidence of this

material. The anomalous behavior of montmorillonite is attributed to its imbibing of the polar organic chemicals used as surfactants into its expandable crystal structure to produce an extremely large basal spacing. This problem can be overcome in some cases by heating the clay to $110^{\circ}C$ for 8 hours, but in other cases this had little or no effect in collapsing the expanded structure.

Even though the project was not a total success, the method holds promise, providing the duration and intensity of the centrifugation is increased and complete purging of polar organic molecules from expandable layered clays can be accomplished.

Density Separation of Clay Minerals

by

Terry Allen Nelsen

A THESIS

submitted to

Oregon State University

in partial fulfillment of
the requirements for the
degree of

Master of Science

June 1971

APPROVED:

Assistant Professor of Oceanography
In Charge of Major

Chairman of Department of Oceanography

Dean of Graduate School

Date thesis is presented *November 30, 1970*

Typed by Marcia Griffin for __Terry Allen Nelsen__

ACKNOWLEDGEMENTS

TABLE OF CONTENTS

LIST OF TABLES

LIST OF FIGURES

LIST OF PLATES AND GRAPHS

DENSITY SEPARATION OF CLAY MINERALS

INTRODUCTION

The separation of clay mixtures into their component minerals would be useful to several scientific disciplines. Soil scientists could refine their knowledge of each mineral's addition to the total cation exchange capacity of a soil. Mineralogists could improve estimates of mineral densities and better study the character of disordered clay structures. Marine geologists could refine provenance and dispersal patterns of marine clays as a result of improved X-ray analysis.

The recognized density ranges of some clay minerals are displayed in Figure 1 (Hurlbut, 1965). Despite considerable overlap, it is probable that in a specific sample at least some of the mineral densities will lie outside the region of maximum overlap and therefore will be amenable to density separation.

To date, success at separation has been limited. Part of the problem lies in the physical size of the material to be studied. The size range of clay minerals is commonly less than 2μ. Because of this small size, optical identification and hand picking are not feasible, and methods depending on other properties of the particles must be employed.

One such property is external electrical charge. Electrophoresis has normally been employed as the technique utilizing external

ρ (g/cm^3) Kaolinite   Illite   Vermiculite   Chlorite Smectites

2. 0 —

2. 2 —

2. 4 —

2. 6 —

2. 8 —

3. 0 —

3. 2 —
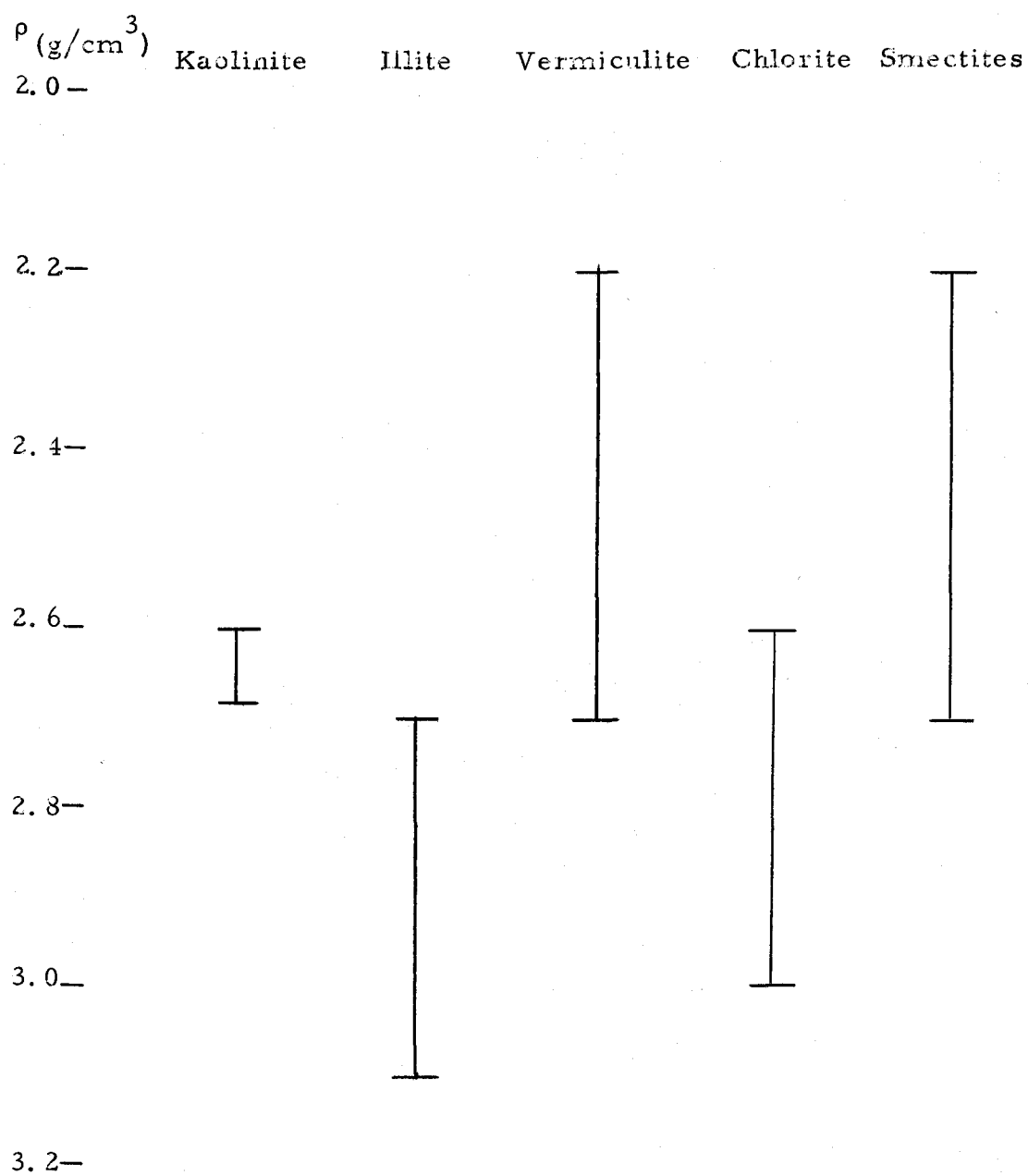
Figure 1. Density ranges of common clay minerals.

electrical charge differences. Thus, McNeal and Young (1963) utilized curtain electrophoresis-paper chromatography. From a three component system of bentonite, kaolinite and vermiculite, only bentonite could be partially isolated after three days of operation. Volk's (1967) work with electrophoresis on an illite-montmorillonite mixture indicated identical mobilities for the two species, and little or no mineralogical variation in the illite.

Another potential property for separating clay species is their density variation. Bock and Ling (1965) made one of the earliest attempts to develop simple gravity-feed heavy-liquid dispensing containers. Although they developed some interesting concepts for dispensing both linear and nonlinear gradients, they made no attempt to put these gradients to practical use. Similarly, Oster and Yamamoto (1963) summarize techniques for preparing density gradients, but did not apply them to specific problems.

Therefore, the object of this study was to investigate the feasibility of separating natural clay mineral mixtures into their fundamental mineral constituents using a density separation technique.

Some previous attempts at heavy liquid separations employed two or more zones of homogeneous density. In some cases, agitation at the interface of two liquids yielded a gradient, whereas in other cases (Woolson and Axley, 1969) several layers were added to a vessel and left as a 'stair-step" gradient. Francis et al. (1970)

developed a density gradient dispensed from syringes which were emptied by computer-controlled cams.

Because of one drawback or another, none of these methods were found suitable for the present study. Some were not reproducible, while others yielded nonlinear gradients, took a great length of time, or were unduly complicated. Instead, use was made of a simple and rapid method for preparing a linear density gradient developed by Halma (1969a). His method is based on simple gravity feed of common laboratory heavy liquids. It yields a density gradient which is both linear and reproducible. A variety of end members can be chosen so that the density range is variable.

METHODOLOGY

Halma (1969a) modified an earlier concept of vessels effluxing a chemical concentration gradient by gravitational leveling (Bock and Ling, 1954) to one which effluxed a density gradient. The basic concept involves the drainage of mutually inverted but similar "pie-wedge" shaped prisms, "a" and "b", into a common efflux tube joined by a "T-joint" (Plate 1a). The hydrostatic head developed by the inverted prism containing the denser end member ("a") is counteracted by tilting that prism a calculated amount (Appendix I), as shown in Plate 1b. This calculated tilt is valid only for pure end members as explained in Appendix I. The amount of liquid draining from each container at any instant is proportional to the cross-sectional area of the meniscuses. Since the prisms are of similar shape, and are mutually inverted, the liquid which drains from each, at a linear rate, also changes proportions at a linear rate. The first liquid to emerge will be the heavy end member and the last will be the light end member. The density transition between these two end members is theoretically linear. A mathematical description of the system is presented by Halma (1969a).

For this study, the vessels used were enlarged from the original designed volume of 30 ml to a total volume of 43 ml, so that a greater amount of clay could be processed with each sample
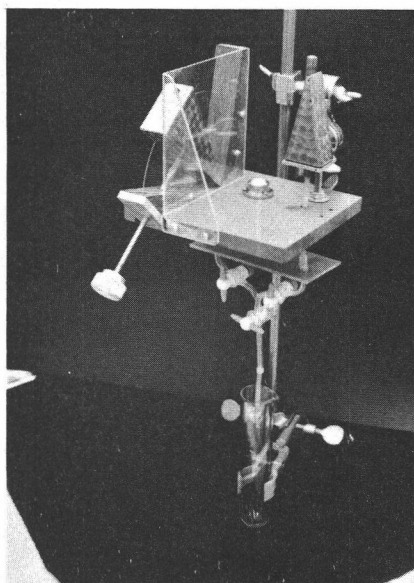
Plate IA

Apparatus used to prepare
heavy liquid density gradients.

Plate IB

Closeup of inverted
prism and tilt
mechanism of A.
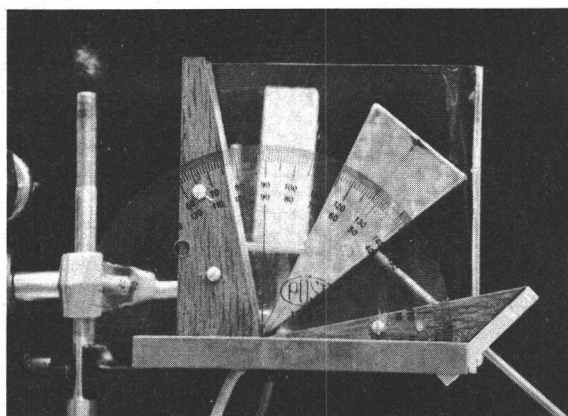
run. Halma's smaller, upright vessel contained a prolonged inlet-
neck for filling and cleaning. This departure from the ideal container
shape causes a deviation from linearity in the density of the effluxed
liquid. To overcome this, the input tube of the smaller vessel was
eliminated and the triangular shape of the container top was retained.
The liquid was introduced through a small hole drilled in the con-
tainer apex where the liquid was delivered by way of a hypodermic
syringe and needle. In addition, Halma's outlet tubes on the bottom
of each vessel were so placed that total drainage from both vessels
was not possible. The unit used in this study allowed for total
drainage from both vessels but changed the level of mixing from the
prisms' base level to a short distance below this level. It was there-
fore necessary to supplement Halma's equation for tilt to compen-
sate for this additional hydraulic head. Appendix II contains a
mathematical description of this modification. In the final analysis
the correction amounted to raising the lighter end member 4.25 cm
for the density ratio ($\rho H/\rho O$) used in this study. Subsequent to
making this correction the linearity of the column was tested and the
data displayed in Graph I. The bulge seen on the lower end of Graph I
results from a hydrostatic imbalance effect between the two end
members. For this particular run there evidently was a slight excess
of the heavy end member present causing it to flood the tube until
hydrostatic equilibrium was reached at the given tilt angle. The end

Graph I. Linearity test of heavy-liquid gradient.

$(n_o - 1)10^4$

$\rho = 2.20$

5300 —

5400 —

5500 —

5600 —

5700 —

$\rho = 2.64$

5800

0   5   10   15   20   25   30   35   cm

∞
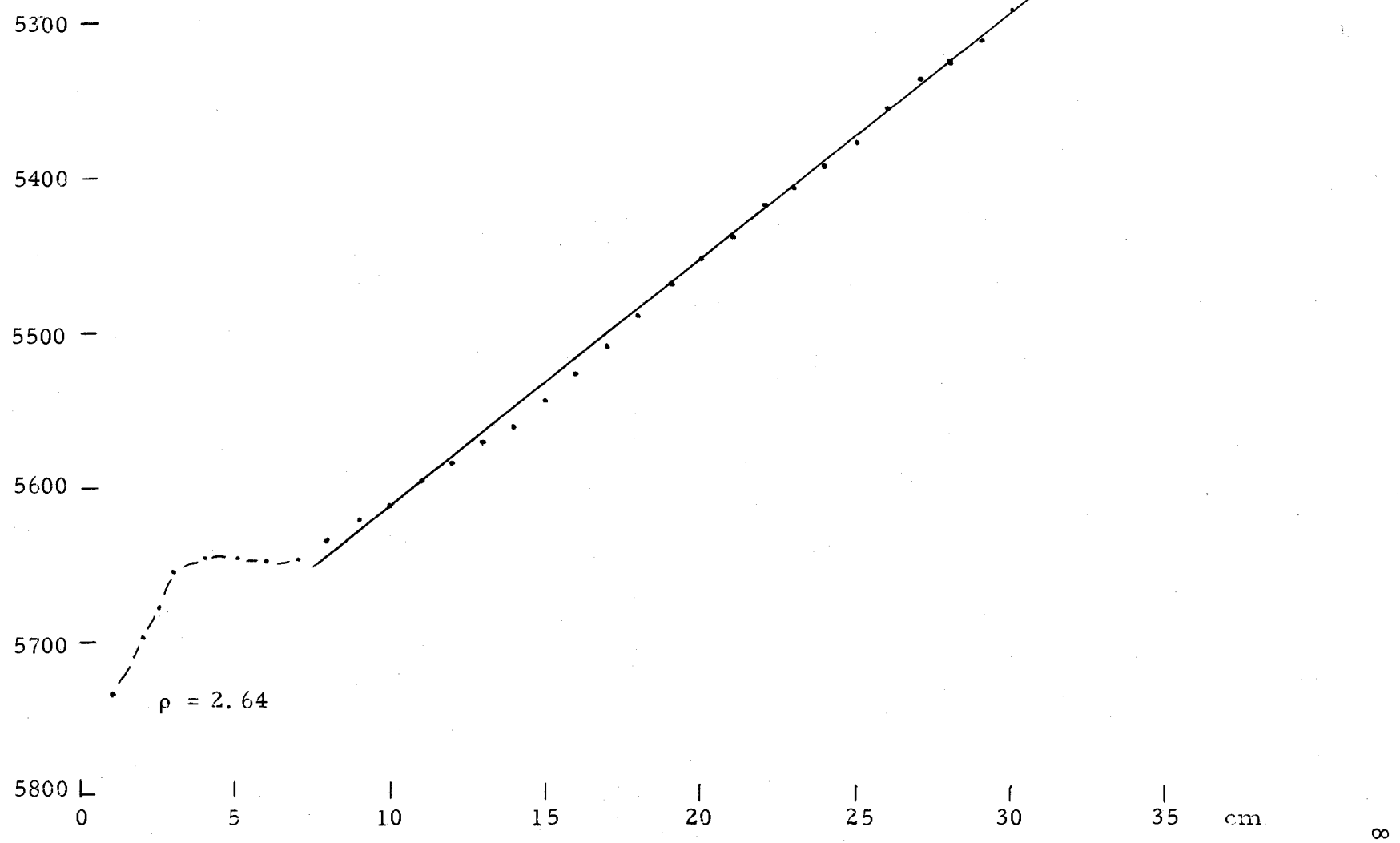
members then effluxed in a linear manner for the rest of the volume.

ANALYSIS OF STANDARD CLAY MIXTURES

The first tests of the method used artificial mixtures of standard clay minerals. Since surface marine sediments rarely contain clays other than illite, kaolinite, chlorite, and montmorillonite, these minerals were used in the mixtures.

Reasonably pure "monomineralic" clay can be obtained from Ward's Scientific Supply Company. Illite #35, illite #36, kaolinite #9, montmorillonite #23, and chlorite #653 were chosen for this study. The two illites were chosen so that variability in this mineral could be investigated.

The standard clays were all processed in the same manner (the procedures are described fully in Appendix III). In short, the clays were ground in n-butanol, washed, Mg-saturated in the case of montmorillonite #23, and then separated into three size fractions, $>2.0\mu$, 2.0-0.5μ, and $<0.5\mu$ by centrifugation (Jackson, 1956). The 2.0-0.5μ size fraction was used in this study because it contains dominantly monocrystalline particles large enough to minimize spinning time for the heavy liquid separation procedure (Pennington and Jackson, 1947).

The standards contained negligible interfering compounds and therefore did not require treatment for the removal of organic matter, free iron, and carbonate. Table I lists the peaks recognized on X-ray

diffractograms of oriented aggregates of the standards. After pro-

cessing, the 2.0-0.5μ fractions of the standards were combined into

the artificial mixtures listed in Table II.

Table I

Mineralogy of Ward's Standard Clays

Illite #35

       Mixed Layer - (Montmorillonite-Illite)
       Chlorite - (002), (004)
       Illite - (001)?, (002), (110), (11$\bar{1}$), (003), (11$\bar{3}$)
       Quartz - (100), (101), (110)
       Feldspar - 3 peaks
       Jarosite - (101), (003), (012), (104), (021), (113), (006), (202)

Illite #36

       Chlorite - (002), (004)?
       Illite - (001), (002), (110), (11$\bar{1}$), (11$\bar{3}$)?, (200)
       Quartz - (100), (101)
       Feldspar - 4 peaks

Chlorite #653

       Chlorite - (001)→ (005), (131), (13$\bar{2}$)

Montmorillonite #23

       Montmorillonite - (001), (004)?
       Muscovite - (002)?
       Pyrophyllite - 1 peak
       Calcite - 1 peak

Kaolinite #9

       Kaolinite - (001), (110), (1$\bar{1}$0), (1$\bar{1}$1), (02$\bar{1}$), (002), (1$\bar{3}$0),
            (1$\bar{3}$1), (1$\overline{31}$)

Table II

Standard Clay Mixtures

Illite #35	39%
Kaolinite #9	45%
Montmorillonite #23	15%
Illite #36	28%
Kaolinite #9	53%
Montmorillonite #23	19%
Kaolinite #9	78%
Chlorite #653	22%

INITIAL CLAY SEPARATION TRIALS

The heavy liquid gradients were prepared from bromoform and carbon tetrachloride. These two non-polar organic heavy liquids were successfully used by Halma (1969a) to isolate clay minerals.

Clay particles tend to undergo severe flocculation in organic liquids. Flocculation agglomerates particles without regard to mineralogy. This can cause particles to get trapped in zones of foreign density and contaminate these zones. Halma (1969a) reports that 2% w/v N- oleyl-1, 3-propylene diamine (Diam-11C) and calcium dodecyl benzene sulphonate (C.D.B.S.) used as surfactants in the heavy liquid column were effective in keeping clays deflocculated. These surfactants were used in this study.

Halma recommended "oleophilizing" the clays by washing aqueous suspensions several times with absolute ethanol, then twice with bromoform, and finally with 2% w/v surfactants. These clay slurries which are still flocculated are then added to the liquid column either by top loading (placing approximately 50 mg of clay on top of the gradient) or by bulk loading (placing the clay sample in either end member before preparation of the gradient). Application of this technique to the present study was unsuccessful due to persistent flocculation of the clay suspensions in the vessels and heavy-liquid columns. The problem was overcome by treating the clays

with surfactant before they were introduced to the heavy-liquids. This allowed the clay particles to be enveloped by the surfactants and not by the organic heavy-liquids. Flocculation was minimized or eliminated with this technique. The details of this procedure are described in Appendix IV.

Because normal gravitational settling requires an excessive amount of time to achieve density separations, samples were separated by centrifugation.

Halma (1969b) reports using relative centrifugal force (R. C. F.) of 33, 000 g at average tube height for a minimum time of 10 hours with a montmorillonite, illite, kaolinite mixture. For this study an International Model SBU centrifuge was used which had a maximum speed of 3400 rpm and a R. C. F. of approximately 3000 at average tube height. Special heavy weight centrifuge tubes were used to avoid breakage due to the load caused by the high density ($\rho \approx 2.4$ average) liquid. Despite this precaution, centrifuge tubes still crushed under the load of top speed centrifugation. After repeated loss of samples due to tube fatigue and failure it was found that tubes rarely crushed when the speed was limited to 2500 rpm (R. C. F. ≈ 2100 g) or less.

Spinning time, at a given speed, appeared to be mainly a function of the sample. In some cases zonation appeared after as little as 1/2 hour. In many cases, good resolution of zones took place in 5-6 hours at 2100 R. C. F., while in a few cases, maximum

zonation took longer than 12 hours.

After zones were produced, they were recovered from the centrifuge tube by a micro-vacuum apparatus. A 20-gauge 6 inch medical spinal needle was bent 180 at the end and attached to a controllable vacuum recovery unit (Figure 2). Once in the collection bottle, the clays were ready to process for X-ray diffraction analysis. The details of the clay extraction and preparation for X-ray analysis can be found in Appendix V.

The samples were X-rayed using a Norelco X-ray diffraction unit equipped with an automatic sample changer and monochromator. Copper radiation was used with a tube voltage of 35 kilovolts and a current of 25 millamps. Divergence and receiving slits were 1° and 0.1mm respectively. The scanning speed for 2°-37° 2θ scan was 1°/minute and was recorded at a chart speed of 2°/inch. A time constant of four seconds was used in all cases.
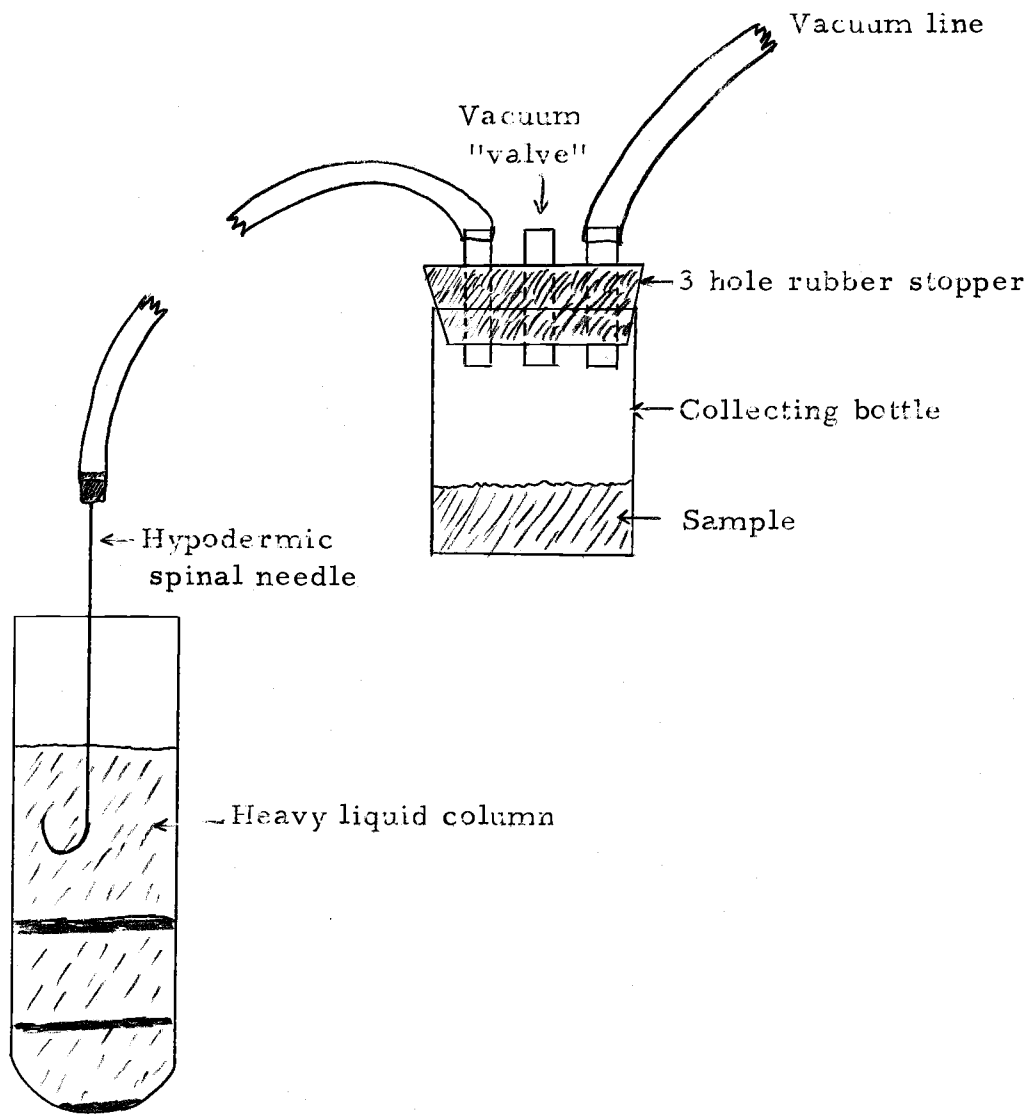
Figure 2.   Unit to recover density layers.

ANALYSIS OF NATURAL CORE SAMPLES

To supplement the data derived from artificial mixtures of standard clays an attempt was made to separate the clay minerals in natural marine sediments. Five samples were taken from a turbidite sequence in a core collected off the Oregon coast. These samples had previously been studied by J. Phipps as part of a larger investigation. The position of samples in the core and previous X-ray analytical data are summarized in Table III.

Although the Ward's standard clays were separated without chemical cleanup treatments, the natural core samples were prepared according to the procedures listed in Appendix VI. The heavy liquid and X-ray treatments of these samples were identical with those for the standard clay mixtures.

Table III

Core 6908-5

Sample	Depth in Core	Mont.	Clay Content (%) Ill.	Chlor.
P33T	124 cm	30	34	35
P34T	135 cm	30	36	34
P35T	145 cm	29.5	35	36
P36T	155 cm	32	31	37
P37T	165 cm	35	29	36

MINERAL IDENTIFICATION

The clay minerals used in this study -- montmorillonite, illite, chlorite, and kaolinite -- were identified from the angular positions of diffracted X-ray maxima, more commonly known as peak positions. Both basal (001) and non-basal ($h$kl) peak positions were utilized for identification. Because of the quality of the diffractograms resulting from the fast scanning speed used in this study, no intra-group identifications were attempted. Although clay minerals are the primary crystalline constituents of fine-grained marine sediments, other minerals such as feldspars and quartz are present in this size fraction and they were identified whenever possible. Table IV lists the minerals identified and the criteria used for the identifications. These criteria are from published (Brown, 1961; Johnson and Vand, 1966; Grim, 1968; Jackson, 1956) and unpublished (Heath, 1966) sources. The identification of mixed-layered clays was based on work by Weaver (1956) and Brown and MacEwan (1950).

Table IV

Criteria for X-Ray Identification of Minerals

Montmorillonite (Mg-Saturated)

$^\circ 2\theta$	5.7
(hkl)	(001)

Montmorillonite (Glycolated)

$^\circ 2\theta$	4.9-5.0
(hkl)	(001)

Chlorite

$^\circ 2\theta$	6.2	12.5	18.8	25.1	31.5
(hkl)	(001)	(002)	(003)	(004)	(005)

Illite

$^\circ 2\theta$	8.8	17.8	19.9	20.9	26.7	33.2
(hkl)	(001)	(002)	(110) (020)	(11$\bar{1}$)	(003)	(11$\bar{3}$)

Kaolinite

$^\circ 2\theta$	12.4	19.9	20.4	21.3	23.1	24.9	35	35.5	36
(hkl)	(001)	(110) (020)	(1$\bar{1}$0)	(1$\bar{1}$1)	(02$\bar{1}$)	(002)	(1$\bar{3}$0)	(13$\bar{1}$)	(1$\bar{3}$$\bar{1}$)

Table IV Continued

Amphibole

$^{o}2\theta$	10. 4-10. 5	31. 7
(hkl)	$(1\bar{1}0)$	(330)

Quartz

$^{o}2\theta$	20. 9	26. 7	36. 5
(hkl)	(100)	$(10\bar{1})$	$(1\bar{1}0)$

Feldspars (few of many peaks)

$^{o}2\theta$	27. 4-27. 9	29. 5	31. 7
(hkl)	(002)	$(1\bar{3}1)$?	(131)?

Calcite

$^{o}2\theta$	29. 2
(hkl)	$(2\bar{1}1)$

Jarosite

$^{o}2\theta$	14. 9	15. 5	17. 5	25. 3	28. 7	29	31. 3	35
(hkl)	$(1\bar{0}1)$	(003)	$(0\bar{1}2)$	$(1\bar{0}4)$	$(0\bar{2}1)$	$(1\bar{1}3)$	(006)	(202)

INTERPRETATION OF DIFFRACTOGRAMS

The following interpretation of X-ray diffractograms is limited, in many cases, as a result of fast scanning speed, small sample volumes yielding diffraction peaks barely above background, and uncertainties in the exact position of diffraction peaks. As a result, the peak positions are accurate only to 0.1^O 2θ at best. Peak heights and peak-height ratios rather than peak areas were used to estimate abundances from the lower quality records.

Standard Minerals

Ward's chlorite #653 was placed in a density gradient and upon centrifugation yielded three layers. The components of these layers are listed in Table V-A and the diffractograms are shown in Figure 3. The top layer (a) of this sample shows the first four orders of the basal spacing (001) whereas the second (b) and third (c) layers show up to fifth order basal spacing as well as some non-basal (hkl) spacings. It is assumed that (hkl) spacings result from non-parallel orientation of the clay particles. This is most likely a result of cementation of particles by carbonates detected in both of the lower layers.

In an attempt to further define the components of the three layers, half-height widths, and structure factor (1F1) ratios were calculated.
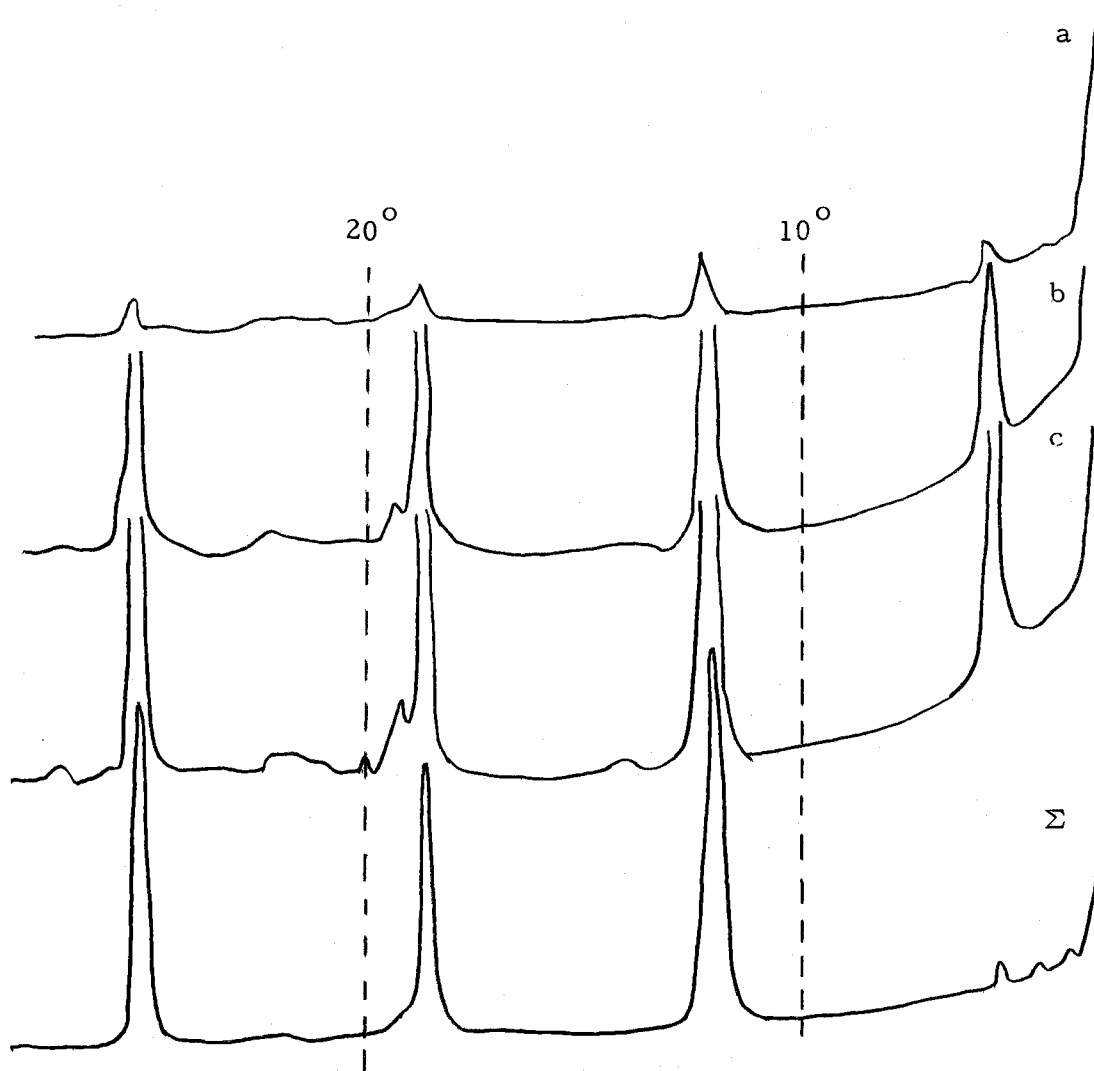
Figure 3. X-ray diffractograms of chlorite #653 and density
layers.

Table V

A - Chlorite #653 - Components of Density Layers

Layer a (top)

Chlorite - (001), (002), (003), (004)

Layer b (middle)

Chlorite - (001), (002), (003), (004), (005), (131), (13$\bar{2}$)

Dolomite - 3 peaks

Layer c (bottom)

Chlorite - (001), (002), (003), (004), (005), (131), (13$\bar{2}$)

Dolomite - 3 peaks

B - Chlorite Peak Half-Height Widths (30ths of an inch)

	(001)	(002)	(003)	(004)
Σ	2.8	5.0	4.2	4.5
a	5.5	4.9	6.5	5.0
b	4.5	4.5	3.8	4.0
c	4.0	3.5	3.6	3.8

The half-height widths are tabulated in Table V-B. The trend of increased "peakedness" is seen from layer "a" to layer "c". Peak broadening is a function of both particle size and crystallinity. Since the heavy-liquid gradient theoretically separates on the basis of density and not size, it is concluded that layers "a" to "c" result from increases in density resulting from increases in particle crystallinity. First and third order peaks of ferruginous-chlorites are very weak (Brown, 1961). To detect any compositional change in the layers, structure factors (1F1) were computed for the various peaks and their ratios were calculated. Comparison of this compositionally sensitive parameter to known compositions (Brown, 1961) revealed no trends.

Illite #35 dispersed into three layers. The components of these layers are recorded in Table VI. Data for the three layers of illite #36, are recorded in the same table. Differences between the two are apparent. Only illite #36 shows mixed layer components and quartz in more than one layer. The appearance of a phase of invarient density, such as quartz, in more than one layer probably reflects incomplete segregation of small grains during centrifugation. The same may be true of the three layers of illitic material. Alternatively, illites of different densities may reflect the breakup of a mixed layered structure of the type shown in Figure 4. This represents a regular mixed-layer structure of species "A" followed by

three layers of species "B" per unit, giving an overall composition of 25% "A" and 75% "B" for the total unit. Random mechanical breakdown of this structure yields six unique density groups of "A" and "B" layers. The hypothetical divisions and their group densities, assuming a density of 2.2 g/cm^3 for layer "A" and 2.6 g/cm^3 for layer "B" are shown in Figure 4.

Table VI

Components of Density Layers of Standard Illites and Kaolinite

Illite #35

I_1 (top)

Illite - (001), (110), (003)
Chlorite - (002)

I_2 (middle)

Illite - (001), (002), (110)
Chlorite - (002), (003)
Quartz - (100), (101), (110)
Feldspar - 2 peaks

I_3 (bottom)

Quartz (101)?

Illite #36

I_1 (top)

Mixed Layer - (75% illite, 25% montmorillonite)
Illite (110), (003), (112), (200, 13$\bar{1}$)
Quartz (100), (101)

Table VI Continued

<u>Illite #36</u>

I_2 (middle)

Mixed Layer - (80% illite, 20% montmorillonite)
Illite - (001), (110)
Quartz (100), (101)
Jarosite - (012), (021), (113)
Feldspar - 1 peak

I_3 (bottom)

Illite - (001), (110), (11$\bar{3}$)
Quartz - (100), (101), (110)
Jarosite - (101), (003), (012), (110), (104), (021), (113),
(202), (006), (024)
Feldspar - 1 peak

<u>Kaolinite #9</u>

K_1 (top)
Kaolinite - (001), (110), (11$\bar{0}$), (1$\bar{1}$1), (002), (1$\bar{3}$0), (13$\bar{1}$),
(13$\bar{1}$)

K_2 (top middle)

Kaolinite - (001), (110), (1$\bar{1}$0), (1$\bar{1}$1), (02$\bar{1}$), (002), (1$\bar{3}$0),
(13$\bar{1}$), (13$\bar{1}$)

K_3 (bottom middle)

(Fraction too small to recover)

K_4 (bottom)

(Fraction too small to recover)

Figure 4

Hypothetical Mixed Layer Clay

Group Densities (g/cm^3)

A = 2.20 g/cm^3

B = 2.60 g/cm^3

A	
B	ρ = 2.40
B	ρ = 2.60
B	
A	ρ = 2.46
B	
B	
B	
A	ρ - 2.50
B	
B	
B	
A	ρ = 2.52
B	
B	
B	ρ = 2.60
A	ρ = 2.20
B	

etc.

Illite #36			Hypothetical Clay
	Layers	Density Ranges	Density "Layers"
ρ = 2.20	0mm	ρ = 2.20	ρ = 2.20
	54mm	ρ = 2.48	ρ = 2.46
85mm			
	58mm	ρ = 2.50	ρ = 2.50
	60mm	ρ = 2.51	ρ = 2.52
ρ = 2.64	85mm	ρ = 2.64	ρ = 2.60

The groups are arranged in order of descending densities in the lower right hand portion of the figure. Data collected during the spin-down of illite #36 showed zones at 0-54mm, 58-60mm, and 85mm from the top in an 85mm long tube. Assuming that the gradient is approximately the same for each column, data from Graph I indicates that the top of the column is 2.2 g/cm^3 and the bottom is 2.64 g/cm^3. Interpolating the densities of the known layer positions into the assumed density range yields the values recorded in the lower left-hand portion of Figure 4, which may be compared with the model values. The match is quite good, giving credence to the model. Further support is gained from the character of the mixed-layer peaks of illite #36. Comparison with published examples of mixed-layer clays (Brown and MacEwan, 1950) shows that illite #36 contains approximately 25% montmorillonite and 75% illite -- values in accord with the hypothetical model.

Two zones of the kaolinite dispersion were too minute to recover. The quality of diffractograms of the other two is inadequate to define the detailed character of these layers (Table VI). It can only be assumed that they also result from density differences resulting from variations in crystallinity.

The standard montmorillonite #23 formed only one layer at the top of the column. X-ray diffraction analysis of this layer showed no well defined peaks. Interaction of the montmorillonite

and the organic chemicals used to disperse the clay is thought to have produced extreme dilation of the expandable layers. This problem is discussed later in the paper.

Mixtures of Standard Minerals

Quantitative estimates of kaolinite and chlorite in mixtures are complicated by the coincidence of first order kaolinite and second order chlorite peaks in X-ray diffractograms. Figure 5 shows the diffractograms of such a mixture and of the two layers obtained from this mixture after centrifugation in a density gradient. Because of the poor quality X-ray diffractograms for this known (chlorite 22%, kaolinite 78%) mixture of Ward's standards, peak heights were used for quantitative estimates rather than peak areas. For the total mixture diffractogram (Σ), this technique yielded concentrations within a few percent of the known values. It was therefore considered a valid method for estimating abundances. The application of this technique to the density splits indicated that the top layer ("A") contained 15% chlorite and 85% kaolinite whereas the bottom layer ("B") contained 29% chlorite and 71% kaolinite. Clearly, a complete separation of these two minerals did not take place.

A three component mixture of Ward's standard kaolinite #9 (45%), montmorillonite #23 (16%), and illite #35 (39%) was made and separated in a density gradient. Three layers resulted and their

Figure 5. X-ray diffractograms of chlorite #653 - kaolinite #9
mixture and density layers.

diffractograms, as well as that of the total mixture, are shown in Figure 6. The top layer ("A") contains montmorillonite (16. 7%), kaolinite (11. 3%), and mixed-layer material (62%). The quantitative estimates were made using conventional weighted peak-area percentages (Biscaye, 1964) with the assumption that the mixed-layer material can be treated as a true illitic component of the mixture. Layer two ("B") contains illite (33%) and kaolinite (69%). The bottom layer ("C") shows the presence of illite and koalinite but no quantitative estimates were made due to the poor quality of the diffractogram. It is clear from this data that no pure mono-mineralic separations were made, but that the top layer ("A") contained essentially all the montmorillonite of the sample.

Natural Marine Sediments

Core samples designated P33T, P34T, P35T, P36T, and P37T supplied by Mr. James Phipps were used for this part of the study. Samples P35T and P37T will be discussed in detail while the others are summarized in Table X at the end of the section.

The data for P35T is summarized in Table VII. Diffracto-grams of the top ("A"), middle ("B"), and bottom ("C") layers, the total sample (Σ), and the glycolated total sample (Σ + GLY) are shown in Figure 7.
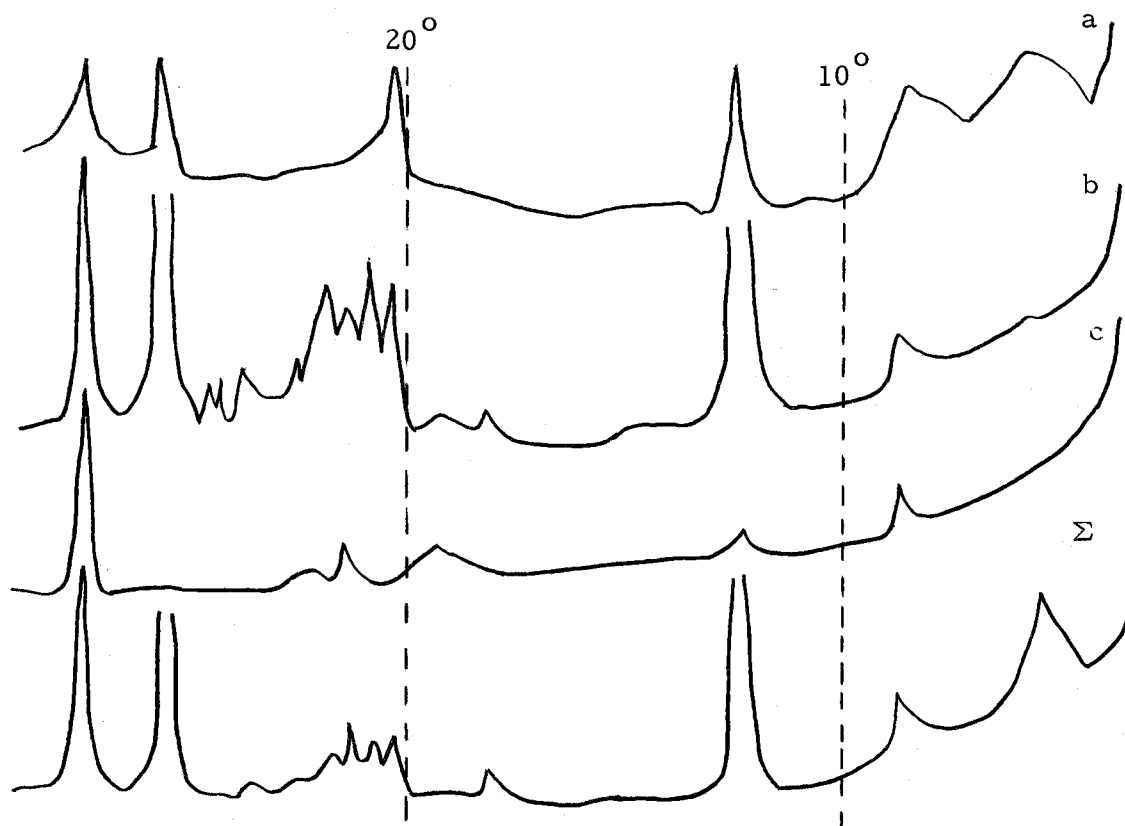
Figure 6.   X-ray diffractograms of kaolinite #9 -
montmorillonite #23 - illite #35 mixture and
density layers.

Table VII

A - Components of Density Layers of Mg-Saturated Sample P35T

Top Layer ("A")

    Mixed Layer
    Illite - (001), (110), (003)
    Chlorite - (002), (003), (004)
    Feldspar - ?

Middle Layer ("B")

    Illite - (001), (002), (11$\bar{1}$), (003), (20$\bar{2}$)?, (131)?
    Chlorite - (002), (003), (004)
    Quartz - (100), (101), (110)
    Feldspar - 6 peaks

Bottom Layer ("C")

    Illite - (001), (002), (110), (11$\bar{1}$), (003), (200)?, (13$\bar{1}$)?, (20$\bar{2}$)?,
        (131)?
    Amphibole - (?), (330)
    Chlorite - (002), (003), (004), (131), (20$\bar{2}$)
    Quartz - (100), (101), (110)
    Feldspar - 8 peaks
    Hornblende - 1 peak

B - Illite Peak Ratios

	"A"	"B"	"C"
$I \dfrac{(002)}{(001)}$	----	0.625	0.595
$I \dfrac{(003)}{(001)}$	2.33	0.765	----

C - Relative Illite and Chlorite Abundances

ID	$\dfrac{x}{Q_{(100)}}$	$\dfrac{x}{Q_{(100)}}$	$\dfrac{x}{Q_{(100)}}$
I (001)	∞	0.58	0.87
C (002)	∞	0.95	2.27

Figure 7. X-ray diffractograms of P35T and density layers.

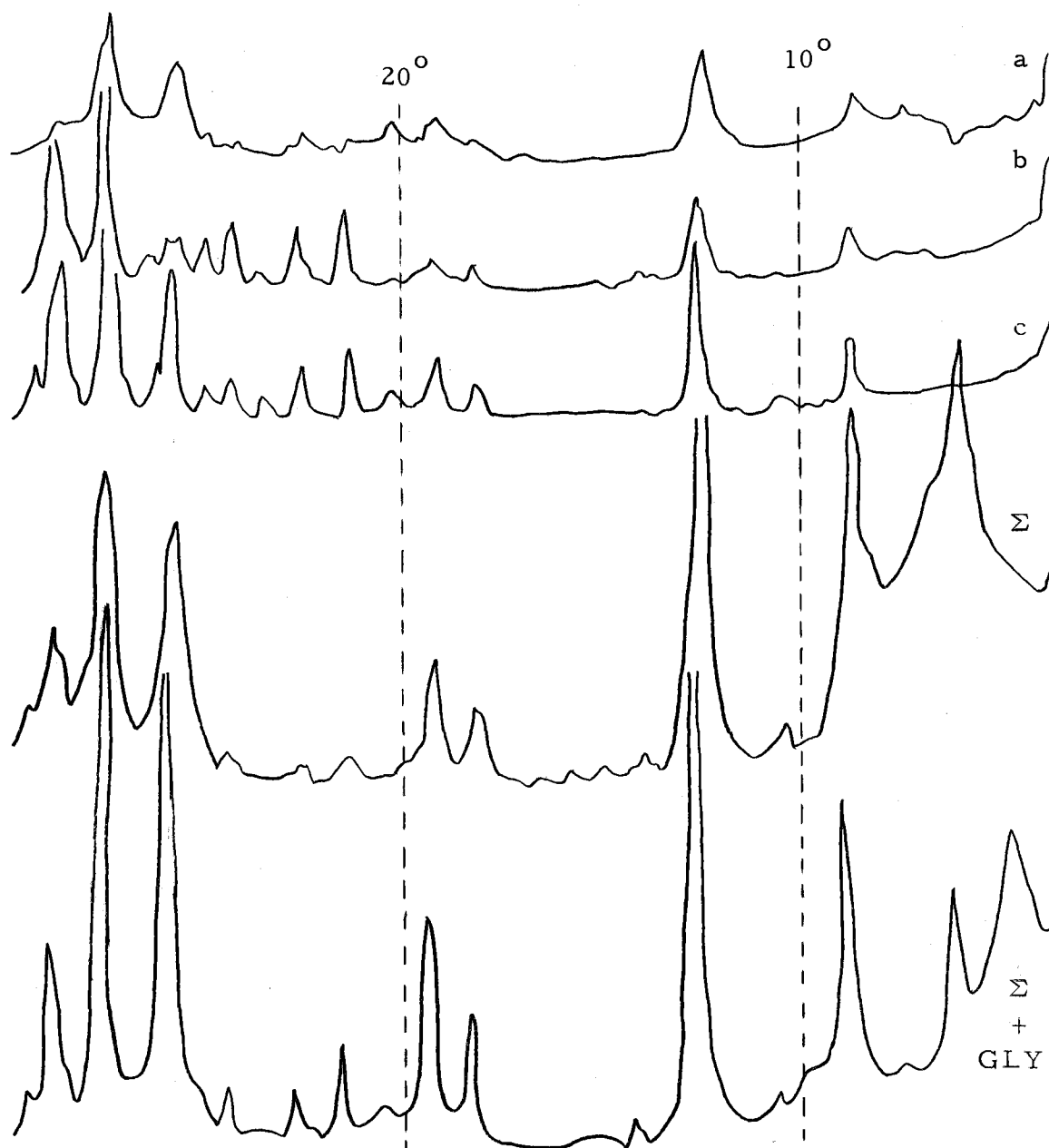The character of the diffractograms from layers "A" to "C" is transitional. Mixed-layer components are found almost exclusively in layer "A", with but a trace amount detected in layer "B". Chlorite and illite appear in all three layers. Again, quartz is found in more than one layer, suggesting that the material found in layer "B" was still in transit to the lower zone. Feldspar is also found in two layers, but amphibole is found only in the bottom layer. No montmorillonite is indicated in any layer. Diffractograms of the glycolated total sample (Σ + GLY) reveal illite, chlorite, and montmorillonite in the low 2θ angle region. The anomalous behavior of montmorillonite is discussed later. The greater number of non-basal (hkl) reflections from phyllosilicates in layers "B" and "C" is attributed to non-ideal orientation of clay minerals resulting from the presence of non-phyllosilicates.

In an attempt to detect a transition in character of the illite peaks in the three layers peak ratios were calculated and recorded in Table VII-B. The abundances of illite and chlorite relative to quartz are calculated as a ratio of clay peak heights to quartz (100) peak height and recorded in Table VII-C.

The data of Table VII-B shows a general trend for the relative increase in magnitude of the illite (001) peak to the (002) and (003) peaks with depth in the tube. In Table VII-C, layers "B" and "C" show an increase in illite and chlorite with respect to quartz.

The absence of quartz in layer "A" makes the ratio values infinitely large and therefore meaningless with respect to the other layers.

The data for sample P37T are tabulated in Table VIII and the diffractograms of the four component layers are shown in Figure 8. Figure 9 is a detailed illustration of the low angle region of Figure 8.

Mixed-layer material of approximately 50/50 $10^O\overset{\circ}{A}$ - $14^O\overset{\circ}{A}$ material is found in layer "A". Mixed-layer material of a slightly different character is found in layer "B". Illite and chlorite are present in all four layers, but the character of their diagnostic peaks changes with depth in the column as seen in Figure 9. Again, in an attempt to detect variations in the character of illite peaks in the four layers, the peak ratios were calculated and are recorded in Table VIII-B. The abundances of illite and chlorite relative to quartz are based on the ratio of their peak heights to the peak height of quartz (100) (Table VIII-C).

The ratios of Table VIII-B show the same trend as those of Table VII-B. The magnitude of the illite (001) peak relative to that of the illite (002) peak increases with depth in the tube. This is interpreted as an increase in crystallinity with depth. In contrast to Table VII-C the bottom two layers of Table VIII-C show a decrease in the abundance of illite and chlorite relative to quartz with depth. Feldspar and quartz are indicated in layer "B", present in layer "C", and obvious in layer "D", but amphibole is restricted to layer "D".

Table VIII

A - Components of Density Layers of Mg-Saturated Sample P37T

Top Layer ("A")

Mixed Layer (random 50/50 mix of 10 $\overset{o}{A}$ & 14 $\overset{o}{A}$ chloritic material)
Illite - (001(, (002), (110), (003)
Chlorite - (002), (003), (004)
Feldspar - ?

Middle Top Layer ("B")

Mixed Layer (illitic and chloritic)
Illite - (001), (002), (110), (003)?
Chlorite - (002), (003), (004)
Feldspar - ?
Quartz - (101)?

Middle Bottom Layer ("C")

Illite - (001), (002)
Chlorite - (002), (003), (004)
Quartz - (100), (101)
Feldspar - 6 peaks

Bottom Layer ("D")

Illite - (001), (002), (110), (11$\bar{3}$), (200), (13$\bar{1}$)
Chlorite - (002), (003), (004), (005)
Quartz - (100), (101), (110)
Feldspar - 8 peaks
Amphibole - (?), (330)

B - Illite Peak Ratios

	"A"	"B"	"C"	"D"
I $\dfrac{(002)}{(001)}$	0.73	0.68	0.64	0.52

C - Relative Illite and Chlorite Abundances

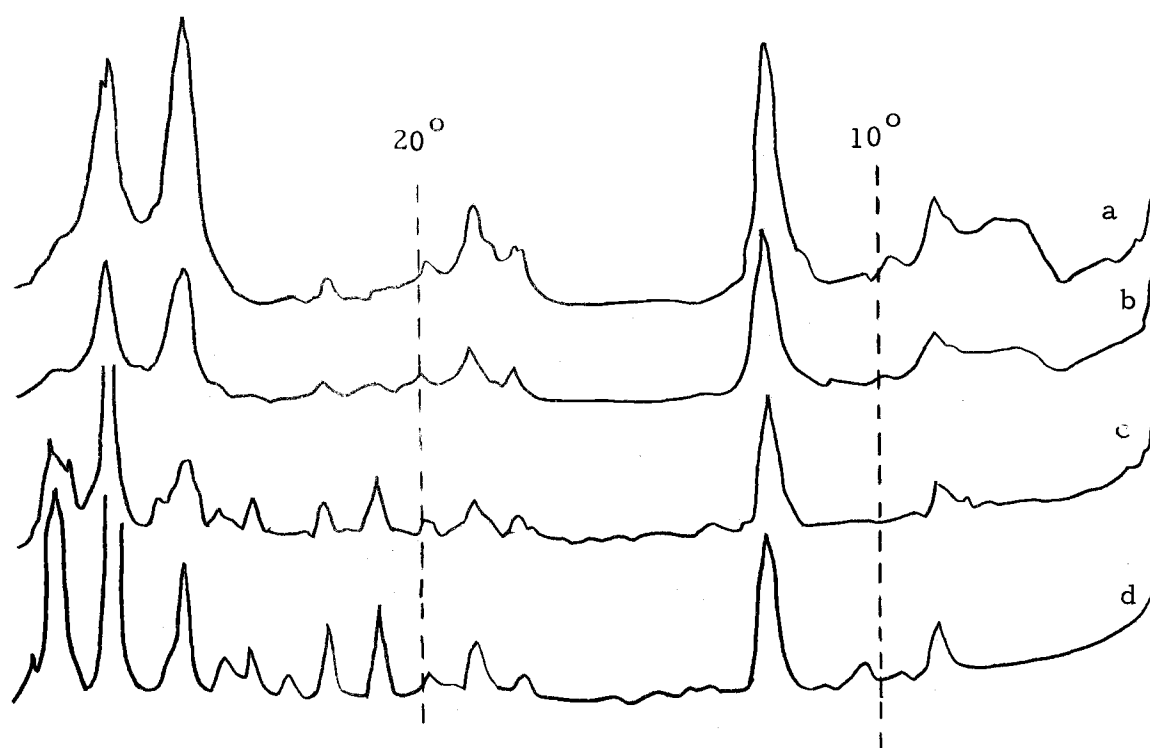|	"A"	"B"	"C"	"D"
I (001)	∞	∞	0.57	0.52
C (002)	∞	∞	1.83	1.54

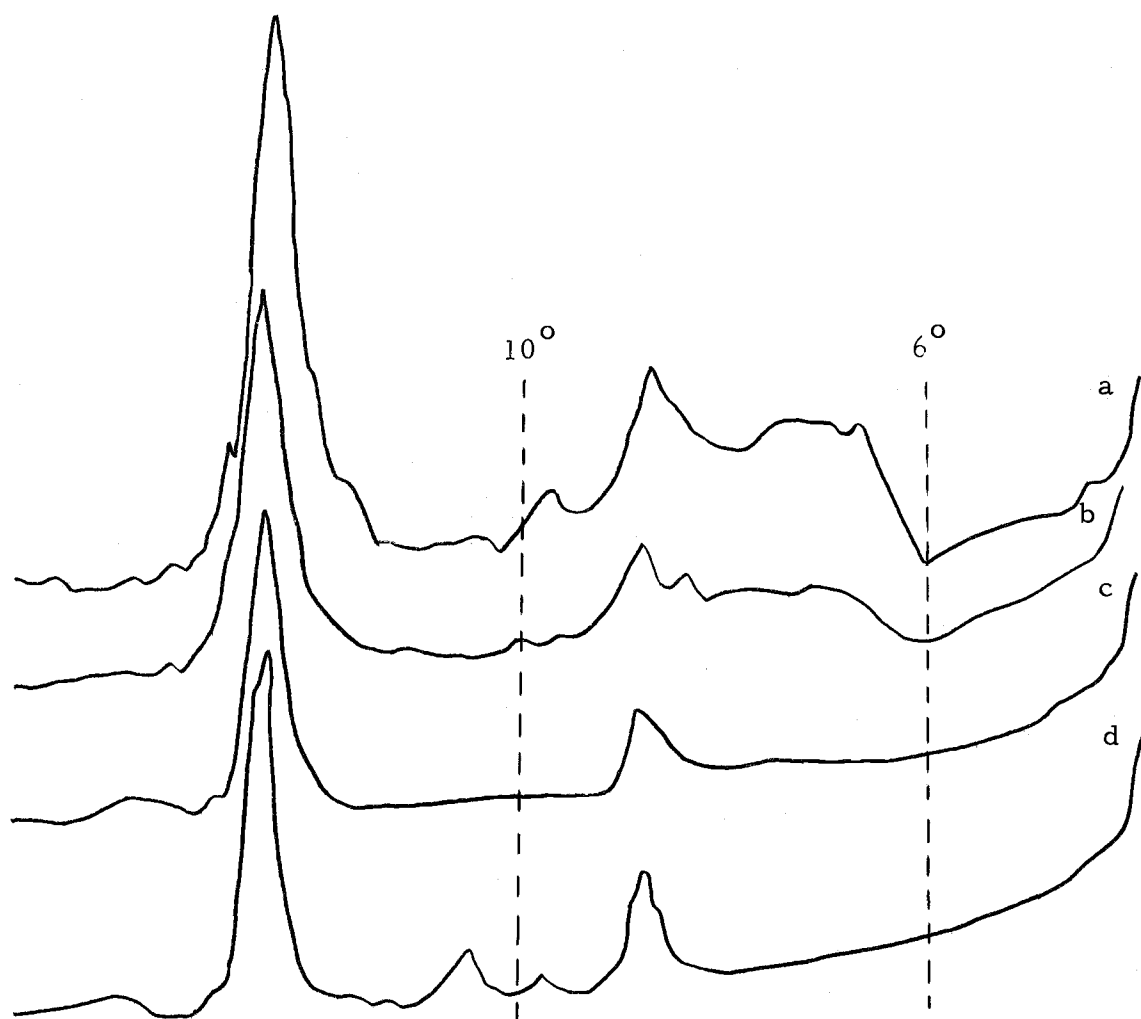Figure 8.   X-ray diffractograms of P37T density layers.

Figure 9. X-ray diffractograms of the low 2θ angle region
of P37T density layers.

Occurrence of the same minerals in several bands probably reflects incomplete separation of material during centrifugation. Montmorillonite was not detected in any layers.

Sample P37T was Mg-saturated prior to analysis. Subsequently, the four sample layers on their planchets were resaturated with a 1 N solution of KCl and X-rayed again. The results of this analysis are tabulated in Table IX and the diffractograms are shown in Figure 10.

Comparison of Figures 9 and 10 shows several mineralogical differences. Mixed-layer material appears to be present in the top three layers of P37T + K but only in the top two layers of P37T. Depending on the exact proportions of the two types of layers, the basal peak of a K-saturated chlorite-intergrade will appear somewhere in the $10\overset{o}{A}$ - $14\overset{o}{A}$ region. As seen in Figure 10, the diffractograms change character within this region from traces "A" to "C". Strong first order chlorite peaks in the $14\overset{o}{A}$ region are more prominent in the K-saturated sample. This difference is most obvious in the two "D" layer traces. Apparently K-saturation of the mounted samples led to the particle reorientation responsible for such a discrepancy as well as for the presence of some non-basal (hkl) peaks not present in the untreated mounts (Table VIII-A). No montmorillonitic material is identifiable in the K-saturated sample.

Table IX

Components of Density Layers of K-Saturated Sample P37T

Top Layer ("A")

>Illite - (001), (002), (003)
>Chlorite - (001), (002), (003), (004)
>Feldspar - ?
>Quartz - (100)?

Middle Top Layer ("B")

>Illite - (001), (002), (110), (020)
>Chlorite (001), (002), (003), (004)
>Feldspar - 1 peak
>Quartz - (100), (101)

Middle Bottom Layer ("C")

>Illite - (001), (002), (110), (020)
>Chlorite - (001), (002), (003), (004)
>Feldspar - 7 peaks
>Quartz - (100), (101)

Bottom Layer ("D")

>Illite - (001), (002), (110), (020), (11$\bar{3}$), (200), (13$\bar{1}$)
>Chlorite (001) → (005), (131), (20$\bar{2}$)
>Feldspar - 7 peaks
>Quartz - (100), (101)
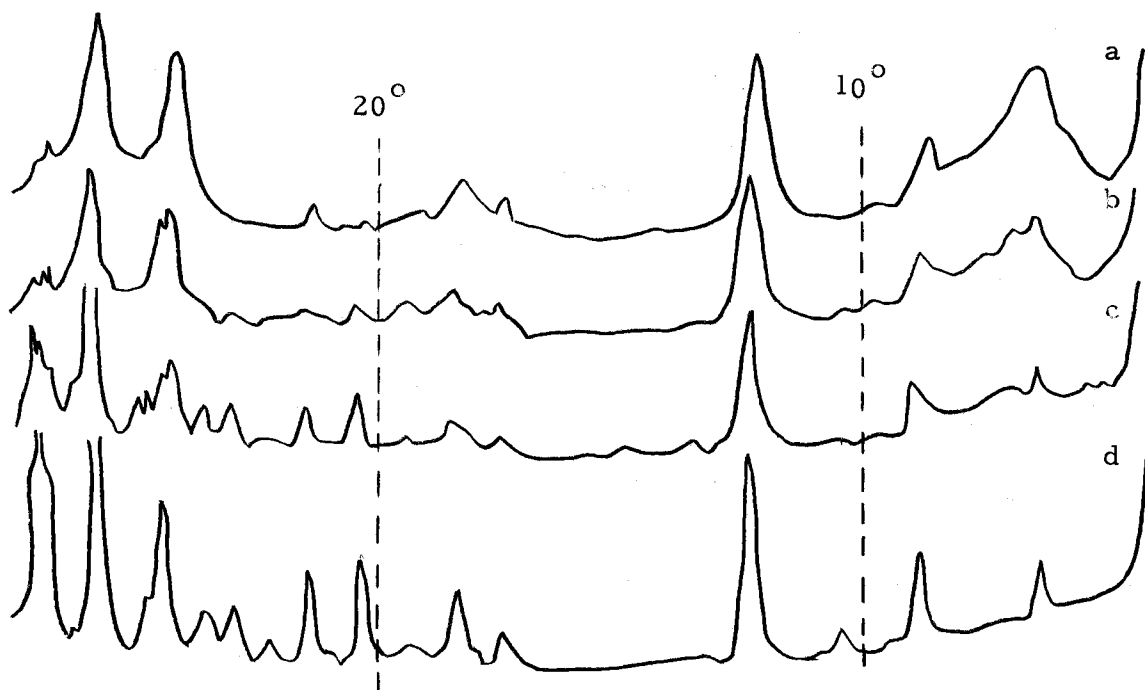>Amphibole - 1 peak

Figure 10.   X-ray diffractograms of K-saturated P37T
density layers.

Table X

Components of Density Layers of Mg-Saturated Samples P33T, P34T, and P36T

A - P33T

    Top Layer
      Illite - (001), (002), (11$\bar{1}$)?, (003)?
      Chlorite - (002), (003), (004)
      Quartz - (100), (101)
      Feldspar - ?

    Bottom Layer
      Illite - (001), (002), (110), (11$\bar{1}$)?, (003)?, (200)?, (13$\bar{1}$)?
      Chlorite - (002), (003), (004), (131)?, (20$\bar{2}$)?
      Quartz - (100), (101), (110)
      Feldspar - 8 peaks
      Amphibole - (110), (330)

B - P34T

    Top Layer
      Illite - (001), (002), (11$\bar{1}$)?, (003)?
      Chlorite - (002), (003), (004)
      Quartz - (100), (101)
      Feldspar - 5 peaks

    Bottom Layer
      Illite - (001), (002), (11$\bar{1}$)?, (003)?
      Chlorite - (002), (003), (004)
      Quartz - (100), (101), (110)
      Feldspar - 7 peaks
      Amphibole - (110), (330)

C - P36T

    Top Layer
      Mixed Layer - (montmorillonite - illite)
      Illite - (001)
      Chlorite - (002)?, (003)?, (004)?
      Quartz - (101)?
      Feldspar - 1 peak?

Table X Continued

C - P36T

    Middle Layer (possibly contamination)
      *Chlorite - (002)?, (004)?, (005)?
      Quartz -)101)
      Feldspar - 1 peak?

    Bottom Layer
      Illite - (001)?, (002)?
      Chlorite - (002), (003), (004)
      Quartz - (100)?, (101)
      Feldspar - 3 peaks
      Amphibole - (110)

*Possibly a high iron chlorite judging by weak (001) and (003) peaks.

SUMMARY AND CONCLUSIONS

The aim of the study -- the isolation of pure minerals from
sedimentary mixtures -- has not been attained. However, several
different polymineralic mixtures of a common density have been
isolated from single samples. The appearance of minerals of in-
variant density, such as quartz, in more than one zone of a density
gradient suggests that the samples were not centrifuged long enough
to reach density equilibrium. An additional complication was intro-
duced by the apparent disappearance of montmorillonite from samples.

All of the natural sediment samples contained approximately
30% montmorillonite (Table III), none of which was detected in the
diffractograms of the various density layers. In many cases thick
spongy masses were extracted from the top of the gradients. A trial
separation using just montmorillonite yielded the same spongy mass
at the top of the column. This mass, after normal clean-up pro-
cedures, yielded a brassy-yellow residue when mounted on a standard
X-ray planchet. The diffractogram of this mount did not show the
presence of montmorillonite. Heating at $110^{\circ}C$ for 8 hours restored
the montmorillonite pattern. One possible explanation for such be-
havior is that the montmorillonite has inbibed organic molecules
into its interlayered structure in the same way that it takes up water
and cations. Cowan and White (1962) showed that exchange of

inorganic cations does take place for large amine ions in mont-
morillonite.   Greenland and Quirk (1962) showed that this exchange
does not involve total replacement.   Brindly and Hoffman (1962)
reported that adsorption as well as exchange took place.   Garrett
and Walker (1962) discovered that the longer the alkyl chain of the
organic molecule, the greater the affinity clay had for it.   They also
stated that when the organic molecule contained chains of 3-4 car-
bons, vermiculite treated with this material swelled in water.   No
swelling took place when the chains were of 8 carbons or greater.
Swelling along the "C" axis was of the order of several hundred
angstroms.   Greenland and Quirk (1962) reported expansion to $42 \overset{o}{A}$
for 250 meq/100g clay (montmorillonite), whereas Garrett and
Walker (1962) found that a high concentration of polar organic mole-
cules did not swell clays beyond about $19.2 \overset{o}{A}$, but low concentration
(0.06 N) caused swelling in water to a basal spacing of $170 \overset{o}{A}$.

The surfactants used in this study were both organic compounds.
The Diam-11C is an amine with high cationic activity and a density
of 0.85 g/cm^3. Since the clays were ultrasonically treated in pure
surfactant and heavy liquids, as well as being cleaned in acetone,
which lowered the surfactant concentration, and finally washed in
water, it would not be surprising if expandable species took up the
polar molecules of the surfactant.   This effect is thought to be re-
sponsible for the "absence" of montmorillonite in the natural core

samples studied. In the test of pure montmorillonite cited above, heating at $110^{\circ}C$ for 8 hours apparently drove off the excess inter-layered polar molecules and restored the normal basal spacing. However, the same heating procedure applied to the natural core samples had little or no effect, suggesting incomplete removal of organic compounds from the clays. In any case, this is a subject for further investigation. If the montmorillonite does take up the low density ($\rho = 0.85$) surfactant, the resulting reduction in density explains why it floats to the surface of the gradient. This effect should be kept in mind as a potentially useful method for extracting montmorillonite from clay mixtures.

Future work in the area of the study should include:

1. Longer centrifuging at higher RCF.

2. Removal of interlayered organics from montmorillonite.

3. Use of internal standard to obtain "weight factors" even if complete mineralogical separations are impossible.

4. Determination of the "optical signature" of zoned samples by variations in transmitted or reflected light.

5. Quantitative recovery of density layers.

6. Detailed investigation of the character of minerals that appear in more than one layer.

7. Extension of the technique to other heavy liquids and perhaps other surfactants.

BIBLIOGRAPHY

Biscaye, P. E. Mineralogy and sedimentation of the deep-sea sediment fine fraction in the Atlantic Ocean and adjacent seas and oceans. Ph. D. thesis, New Haven, Yale University, 1964. 86 numb. leaves.

Bock, R. M. and N. S. Ling. 1954. Devices for gradient elution in chromatography. Analyt. Chem. 26: 1543.

Brindley, G. W. and R. W. Hoffmann. 1962. Orientation and packing of aliphatic chain molecules on montmorillonite. Clays and Clay Min. 9: 546-557.

Brown, G. and D. M. C. MacEwan. 1950. The interpretation of X-ray diagrams of soil clays. Jour. of Soil Sci. I: 239-253.

Brown, G. (Ed.). 1961. The X-ray identification and crystal structures of clay minerals. Mineralogical Soc. of London Pub. 544 pp.

Cowan, C. T. and D. White. 1962. Adsorption by organo-clay complexes. Clays and Clay Min. 9: 459-468.

Francis, C. W., et al. 1970. Separation of clay minerals and soil clays using isopycnic zonal centrifugation. Soil Sci. Soc. Amer. Proc. 34: 351-353.

Garrett, W. G. and G. F. Walker. 1962. Swelling of some vermiculite-organic complexes in water. Clays and Clay Min. 9: 557-568.

Greenland, D. J. and J. P. Quirk. 1962. Adsorption of l-n-alkyl pyridinium bromides by montmorillonite. Clays and Clay Min. 9: 459-468.

Grim, R. E. 1968. Clay mineralogy. McGraw-Hill, New York. 596 pp.

Halma, G. 1969a. A simple and rapid method to obtain a linear density gradient. Clay Min. 8: 47-57.

Halma, G. 1969b. The separation of clay mineral fractions with linear heavy liquid density gradient columns. Clay Min. 8: 59-69.

Heath, G. R. 1966. Unpublished X-ray diffractograms of standard minerals.

Hurlbut, C. S. 1965. Dana's Manual of Mineralogy, 17th Ed. John Wiley and Sons, Inc. New York. 609 pp.

Jackson, M. L. 1956. Soil chemical analysis - advanced course. (4th printing, 1968.) Published by the author, Department of Soil Science, University of Wisconsin, Madison. 894 pp.

Johnson, G. G. and V. Vand. 1966. KWIC guide to the powder diffraction file. ASTM Publ. PD 15-16K.

McNeal, B. L. and J. L. Young. 1963. Paper electrochromatography of clay minerals. Nature 197: 1132.

Oster, G. and M. Yamamoto. 1963. Density gradient techniques. Chem. Rev. 63: 257.

Pennington, S. J. and M. L. Jackson. 1947. Segregation of the clay minerals of polycomponent soil clays. Soil Sci. Soc. Amer. Proc. 12: 452.

Volk, B. G. 1967. Electrophoretic separation of illite and montmorillonite clay minerals. Unpublished M. S. thesis, Ohio State University. 71 numb. leaves.

Weaver, C. E. 1956. Mixed-layer clays in sedimentary rocks. Jour. Sed. Pet. 41: 202-221.

Woolson, E. A. and J. H. Axley. 1969. Clay separation and identification by a density gradient procedure. Soil Sci. Soc. Amer. Proc. 33: 46-48.

APPENDICES

APPENDIX I

Tilt Angle Formula

Halma's equation for reducing the hydraulic head of ρH to zero is:

$$\text{COT} X - \text{COT}(\beta + X) = \frac{2V}{dH_L^2}\left(\frac{\rho H}{\rho L}\right)^2$$

Where:

X = the angle between the more tilted side of the vessel and the horizontal;

β = the angle of aperture of the vessel;
v = the initial volume of liquid in each vessel;
d = the depth of the vessels;
ρH & ρL = the densities of H & L respectively;
H_L = the height of the smaller vessel.

This expands to:

$$\frac{1}{\tan X} - \frac{1 + \tan X \tan \beta}{\tan X + \tan \beta} = \frac{2V}{dH_L^2}\left(\frac{\rho H}{\rho L}\right)^2$$

Solving for "X" obviously reduces to:

$$X = \tan^{-1}\left\{\frac{\frac{2V}{dH_L^2}\left(\frac{\rho H}{\rho L}\right)^2 \tan\beta \pm \left[\frac{4V^2}{d^2 H_L^4}\left(\frac{\rho H}{\rho L}\right)^2 \tan^2\beta - 4\tan^2\beta + \frac{8V}{dH_L^2}\left(\frac{\rho H}{\rho L}\right)^2 \tan\beta\right]^{\frac{1}{2}}}{2\left[\tan\beta - \frac{2V}{dH_L^2}\left(\frac{\rho H}{\rho L}\right)^2\right]}\right\}$$
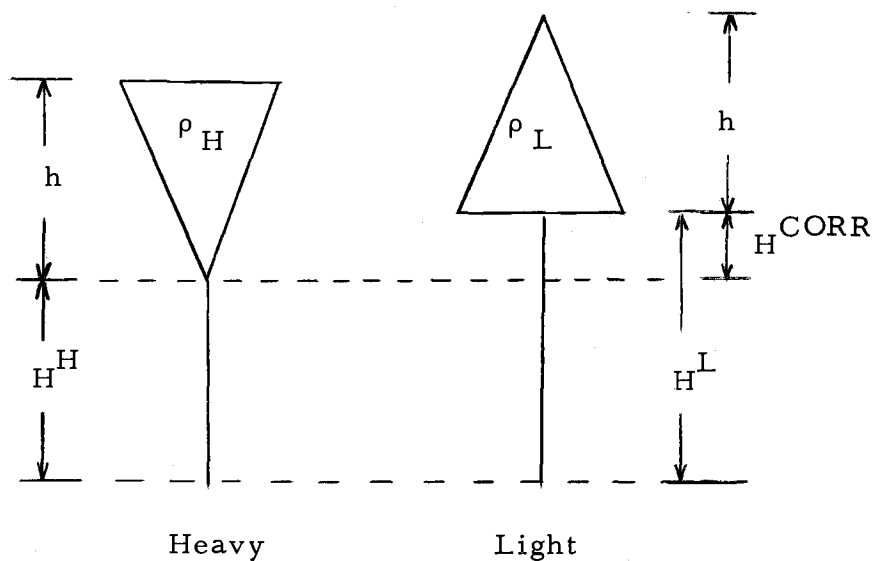
APPENDIX II

Hydraulic Head Correction

Using the basic assumption that hydraulic equilibrium has been established when the following equation is true $H'\rho' = H''\rho''$, where H' and H'' are the heights of the different density liquids (ρ' and ρ'') above a common reference level, the correction for the modified mixing level can be derived.

$$H^H \rho_H = H^L \rho_L$$

$$H^H \rho_H = (H^H + H^{CORR})\rho_L$$

$$H^{CORR} = \left(\frac{\rho_H - \rho_L}{\rho_L}\right) H^H$$

Heavy   Light

APPENDIX III

Processing of Standard Clays

1. Resistant clay blocks are mechanically crushed until they pass through a 63µ screen.

2. Crushed material is wet ground under n-butanol in a Fisher automatic grinder for about four hours to reduce the sample to approximately the clay-size range without damaging the mineral structure.

3. Clay samples are washed free of n-butanol with acetone and centrifuged. This step is repeated three times.

4. The clays are washed with water at least three times to remove the acetone, with the supernatant liquid decanted off after each centrifugation.

5. Each sample is then suspended in water and centrifuged according to Jackson's (1956) formula

$$t_{min.} = \frac{63.0 \times 10^8 \ n \ Log_{10} \frac{R}{S}}{(N_m)^2 \ (D\mu)^2 \ (\Delta\rho)}$$

R = radius (cm) of rotation of top of sediment in tube.

S = radius (cm) of rotation of surface of suspension in tube.

N_m = RPM

$D\mu$ = particle diameter in microns (µ)

η = viscosity of suspension fluid in poises which can be obtained from the Handbook of Chemistry & Physics for any given temperature.

Δ_ρ = different in specific gravity between particle and suspension liquid.

It should be noted here that a low value of N_m was chosen to increase the spinning time of a given size fraction. This was done so that both the positive and negative acceleration times are a small percentage of the total spinning time.

APPENDIX IV

Preparation of Clays for the Heavy-Liquid Gradient

1. The washed, sized, and cation saturated sample is placed in a glass test or centrifuge tube.

2. The surfactants to be added are N-oleyl-1, 3-propylene diamine (Diam-11C) and calcium dodecyl benzene sulphonate (C. D. B. S.). The Diam-11C is heated in a hot water bath until a clear brown solution shows no signs of a precipitate. A hot water bath for the C. D. B. S. lowers its viscosity to a workable range. From these warm surfactants a 50/50 mixture is made. Persistent stirring of the warm surfactants is necessary for the C. D. B. S. to go into solution with the Diam-11C.

3. To a centrifuge tube enough of the surfactant mixture is added to amount to 2% w/v of the total heavy liquid column.

4. To the still warm surfactants of #3 the clay sample is added. Since the viscosity of the surfactants is still quite high, ultrasonic treatment is necessary for complete dispersion of the clay sample. For this study a Bransonic 12 ultrasonic unit was used operating at 60 HZ. Ultrasonic treatment should be minimized due to rupturing of clay crystal structures upon prolonged treatment.

5. The heavy liquid end member chosen for bulk loading is now

added to the clay-surfactant mixture and ultrasonified until

fully mixed.

APPENDIX V

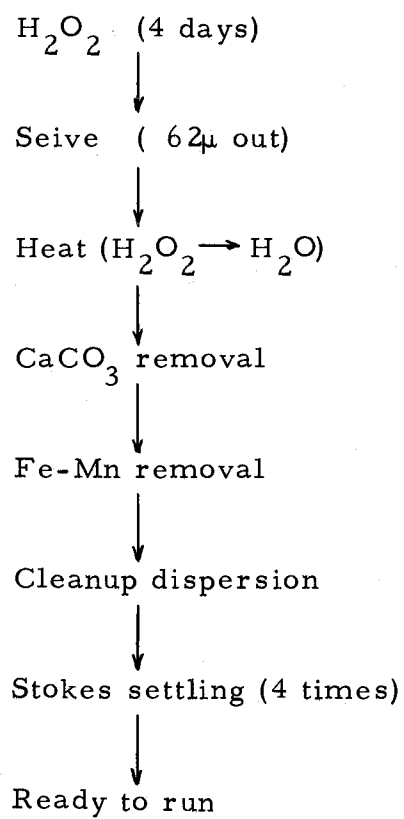## Cleanup of Heavy-Liquid Saturated Clays

1. The layered clays are removed from the centrifuge tubes with the microvacuum apparatus of Figure 3. After each layer is removed, acetone is sucked through into the sample collection tube to assure total sample recovery and to clean the apparatus for the next recovery.

2. With the sample and heavy-liquid in a centrifuge tube, acetone is added as a dilutant.

3. The sample is centrifuged and the supernatant is carefully discarded.

4. Steps 2 and 3 are repeated until the sample is free of heavy liquids.

5. The sample is now washed with water and centrifuged at least three times or until all acetone is removed.

6. The samples are now ready for X-ray analysis.

Preparation of Clays for X-Ray Analysis

1. Porous silver plugs are pressed to 40 ft-lbs pressure in standard Norelco planchets.

2. One ml of sample thoroughly dispersed in water is pipetted
   onto the silver plug to which vacuum is applied. Minimum
   vacuum is used to prevent collapse of the silver plug.

3. Unless glycolation is desired, the sample is ready for X-raying
   after a one hour drying time.

APPENDIX VI

Clay Cleanup Treatments[*]

H_2O_2 (4 days)

↓

Seive (62μ out)

↓

Heat ($H_2O_2 \rightarrow H_2O$)

↓

$CaCO_3$ removal

↓

Fe-Mn removal

↓

Cleanup dispersion

↓

Stokes settling (4 times)

↓

Ready to run

[*]Jackson (1956)